Oral Presentation

The 7th TSME International Conference on Mechanical Engineering
13-16 December 2016

TSME ICOME 2016
Mechanical Engineering Innovation for Green Society

AME0019

Simulation of Multi-cell Thin-walled Structure under Impact Loads with Fracture Damage Mechanism

Chaow Srisuppapakdee[1,*], Pattaramon Jongpradist[1]

[1] Department of Mechanical Engineering, Faculty of Engineering, King Mongkut's University of Technology Thonburi, 126 Prachauthit Road, Bangmod, Thung khru, Bangkok, 10140, Thailand
[*] Corresponding Author: srisuppapakdee@gmail.com

Abstract

In the design of thin-walled energy absorber, finite element simulation is employed to investigate the structural strength and energy absorption behavior under impact as well as to rate the crash performance. Among other profiles, multi-cell thin-walled conical shells exhibit high efficiency in energy absorption. This work aims to employ dynamic explicit finite element analysis including material behavior from fracture damage to predict failure characteristics of multi-cell thin-walled structures under direct and oblique impact loads. Results from two material models; one without material degradation and one with fracture progressive damage evolution due to impact, are compared. When fracture damage is not included, the key parameters in engineering design, such as peak force, mean crushing force and energy absorption capacity can be overestimated. Moreover, the predicted failure modes are different in some cases. Such discrepancies are more evident in multi-cell members with a large number of cell under dynamic impacts in which high plastic strain zones are prominently present. Proper design of multi-cell conical shell as energy absorber is recommended based on buckling failure mechanism, deformation mode and energy absorption responses.

Keywords*:* Multi-cell thin-walled structure; Fracture damage; Impact load; Energy absorption; Finite Element Analysis

1. Introduction

Aluminium thin-walled tubes are widely used as energy absorber in passenger cars due to its high strength to weight ratio and superior structural performance in energy dissipation in relation to its density. For a collapsible energy absorber, the kinetic energy from impact load is conversed into plastic deformation stored as strained energy in the tube. Many researchers have been studied energy absorption capacity and effectiveness of thin-walled tubes with different geometric cross sections subjected to direct and oblique loads [1-3]. The crush characteristics depend on the magnitude of loads, strain rates, deformation patterns and material properties [4].

To further improve the crashworthiness of the aluminum tubes, multi-cell design with considerable number of corners and axial stiffening are experimentally and numerically investigated to promote local folding patterns during impact [5-7]. Metal foam-filled thin-walled structures are also proposed to increase energy absorption under direct impact cases [8-9]. However, the foam-filled multi-cell structures are not effective under oblique loads since global buckling mode dominantly occurs [10]. Tapered tubes exhibit higher energy absorption when subjected to oblique dynamic impact [11-12]. Although truncated circular cones are shown to be suitable as energy absorber due to their stable plastic behavior when subjected to axial impact, studies on their applications are limited. Sheriff et al. [13] optimized conical shells under direct load by varying the semi-apical angle of a conical tube. When the semi-apical angle of the frusta decreases, the tube can better undertake energy absorption from the deformation. Hui and Xiong [14] studied the crashworthiness performance of conical tubes with nonlinear thickness distribution. It was concluded that the material hardening properties and the nonlinear thickness distribution can advance the crashworthiness performance in direct load.

The crash efficiency of conical shells was improved with an addition of foam-filled core [15]. The cones with foam core can withstand a larger degree of oblique dynamic impact before global buckling occurs. Large plastic strains were observed at the impact point and the locations of folding. Nonetheless, in numerical simulation of dynamic impact, fracture damage from excessive plastic deformation is mostly not considered. Hooputra [16] suggested the use of damage evolution including strain rate sensitivities, stress triaxiality and forming limit diagram in the material model for dynamic impact test and showed that the simulated results are in accordance with experimental data.

This research is focused on evaluation of dynamic behaviors of multi-cell conical aluminum tubes under direct and oblique loads based on nonlinear explicit finite element analysis with and without Hooputra damage evolution model. The parameters of interest including initial peak force, mean crushing force, energy absorption, and specific energy absorption, of the single and multi-cell conical tubes are studied and compared.

AME0019

2. Theoretical background

This section describes backgrounds on parameters characterizing the effectiveness of energy absorption for thin-walled member and the concepts for modeling of fracture damage mechanism used in the current study.

2.1 Energy absorption of thin-walled member

When a thin-walled member is subjected to an impact load, the structure mostly collapses in progressive folding to absorb the crash energy. The relationship between force and displacement is as shown in Fig. 1.

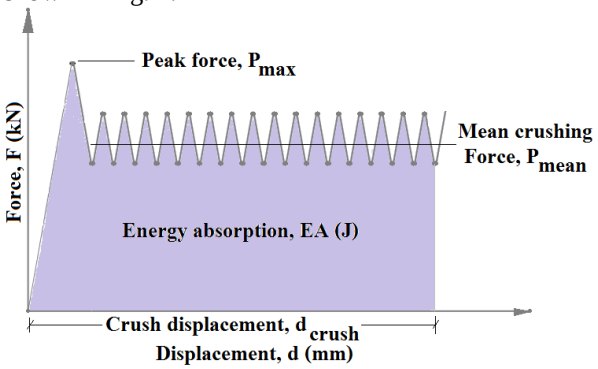

Fig. 1 Force-displacement diagram of thin-walled tube under axial compression

The initial peak force, P_{max} of the column is the initial maximum force that occurs at the beginning of the impact. The mean crushing force, P_{mean} is the average force used in local folding of the member calculated by

$$P_{mean} = \frac{1}{d_{crush}} \int_0^{d_{crush}} F(s)ds \qquad (1)$$

where F is the force during impact, s is displacement and d_{crush} is the total crushing displacement.

The energy absorption (EA) is the total energy absorbed by the structure defined as

$$EA = \int_0^{d_{crush}} Fds = P_{mean} \times d_{crush} \qquad (2)$$

The specific energy absorption (SEA) is the value used to compare the energy absorption per unit mass of thin-walled member obtained from

$$SEA = \frac{EA}{m} \qquad (3)$$

where m is the mass of thin-walled structure. In the design of passenger car's thin-walled energy absorber, the objective is to maximize the specific energy absorption of the member such that the member is able to absorb crash energy by progressive folding of the member. The initial peak force should be kept minimal to alleviate the risk of passenger injuries.

2.2 Fracture damage mechanism

A typical stress-strain response of a metal specimen is depicted in Fig. 2. Initially, the material behaves as linear elastic with steep slope under an increasing load (line a-b). Then, plastic yielding occurs and strain hardening develops (line b-c). Beyond point c, degradation of stiffness due to the initiation and growth of micro-cracks and micro-voids causes reduction of load carrying capacity (line c-d). Material failure is characterized by the complete loss of load carrying capacity of a material unit (point d).

In the modeling of damage evolution, failure mechanism must be defined by four part, i.e., flow curve (line a-b-c), damage initiation criterion (point c), damage evolution law (line c-d) and material failure (point d). Damage initiation criteria for the fracture of metal includes ductile and shear criteria. The ductile criterion is used to predict the onset of damage due to nucleation, growth and coalescence of voids specified by the equivalent plastic strain, stress triaxiality and strain rate. The shear criterion predicts the shear band localization depending on equivalent plastic strain, shear stress ratio and strain rate. For necking instability of sheet metal, forming limit diagram is used to assess damage initiation and the maximum strains that sheet material can sustain are referred to as the forming limit strains.

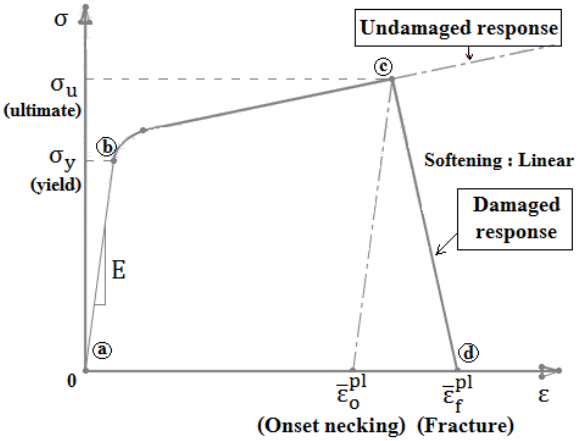

Fig. 2 Elastic-plastic material with progressive damage

Damage evolution must be used in combination with damage initiation criteria to drive the softening of material before fracture damage. The damage evolution law can be specified in terms of equivalent plastic displacement or fracture energy dissipation. Fracture occurs when the material stiffness is fully degraded.

3. Finite Element Model

The FE model is explained in this section. Simulation results are compared and validated with experimental results from previous work.

3.1 Models and conditions

The nonlinear dynamic explicit finite element simulation of circular tapered tubes under direct and oblique loads is performed to study collapse behavior of thin-walled structure and effects of thin-walled structure under high velocity impact. The models are single-cell and multi-cell thin-walled conical shells with length of 180 mm and outer diameters on top and bottom sections of 60 and 80, respectively. The shell is constrained to a fixed base and crashed by a rigid wall

of mass 275 kg with initial velocity of 15 m/s as shown in Fig. 3. Self-contact interaction is also specified at the tube surfaces. Friction coefficient for all contact surfaces are set at 0.15. From mesh convergence study, the mesh size of 2 mm is efficient.

The model name is defined as TL*x*N*y* where T means tapered tube model, *x* indicates the number of inside layer, and *y* is the number of cell along the shell perimeter. In this study, the specimens of interest are single-cell and multi-cells with one to three inside layers and the numbers of cell along the circumference vary from four to eight. An example of TL2N6 model which is a tapered cone with two inside layers and six cells along the tube perimeter is shown in Fig. 4.

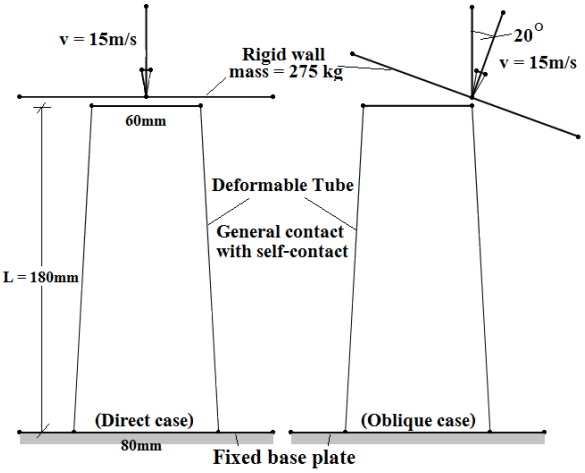

Fig. 3 loading conditions in finite element simulation

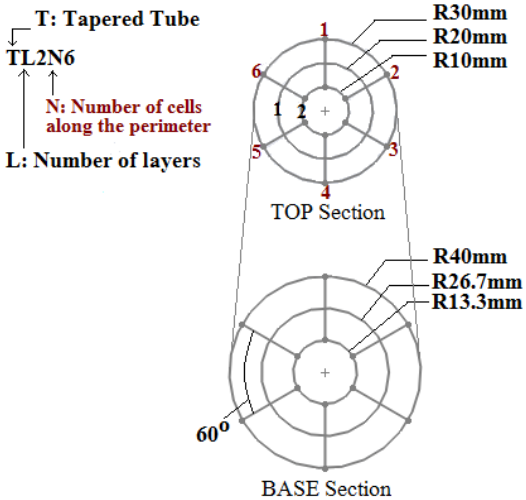

Fig. 4 TL2N6 multi-cell model

3.2 Material properties

The finite element (FE) models are extrusions made from aluminium alloy EN AW7108-T6 with Young's modulus of 70 GPa and Poisson's ratio 0.33. Two material models are considered in the current study and results from the two models are compared. Material model A implements stress-strain curves for different strain rates illustrated in Fig. 5 without damage evolution formulation. Material model uses the same flow curves with fracture damage mechanism defined when the equivalent plastic strain exceeds the prescribed value. The ductile, shear, and forming limit diagram criteria for initiation of damage are specified as shown in Fig. 6(a) to (c), respectively. The mesh-independent displacement-based damage evolution is stated by linear softening. The removal of element is set at the plastic displacement of 0.1 mm after the onset of damage.

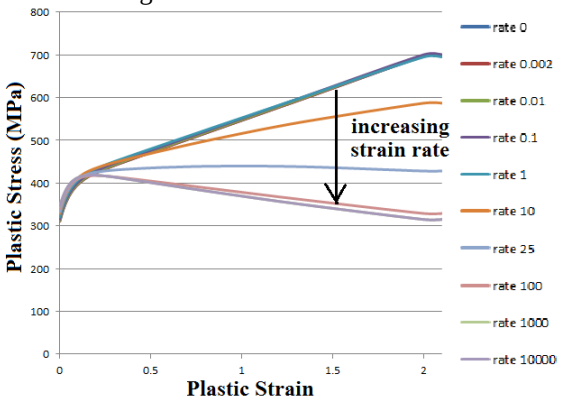

Fig. 5 Stress-strain curve of AW7108-T6

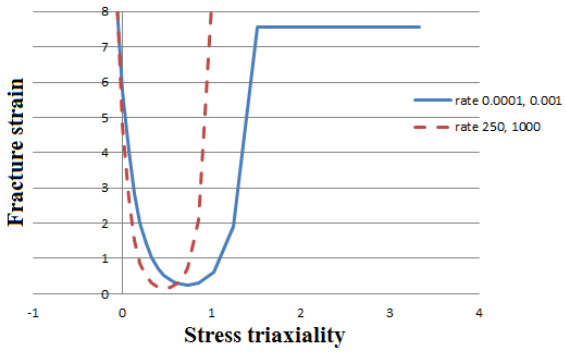

(a)

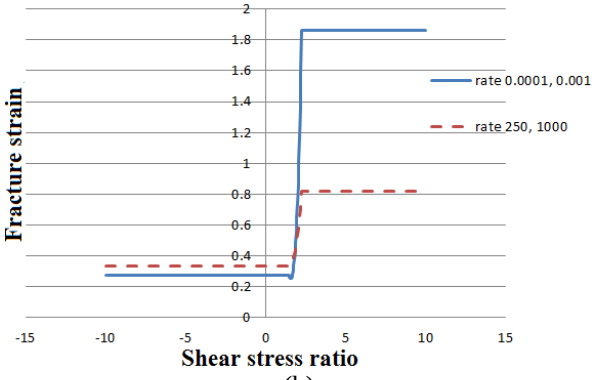

(b)

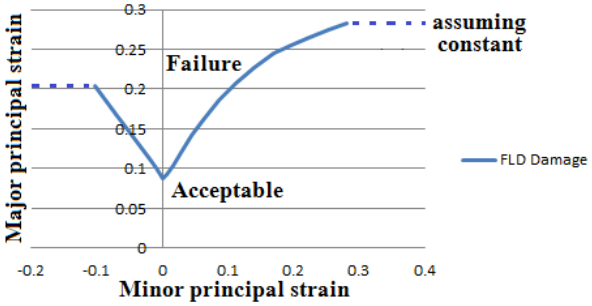

(c)

Fig. 6 Damage initiation model (a) ductile criterion (b) shear criterion (c) forming limit diagram

AME0019

3.3 Validation of FE model

A thin-walled double chambered aluminum extrusion under impact investigated in Hooputra [16] is used to validate the finite element models.

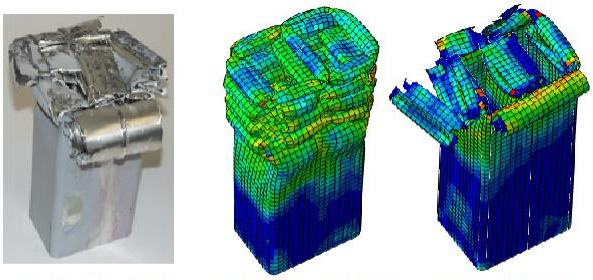

Fig. 7 Failure modes from experiment, FEA without damage evolution and with damage evolution

Table 1 Comparison of experimental results from [16] and FE results.

Results	P_{max} (mm)	d_{crush} (mm)	EA (kJ)
Hooputra [16]	264	192	25.1
FE model without damage evolution	324	194	25.2
FE model with damage evolution	246	195	25.1

The failure modes for the three cases are illustrated in Fig. 7. The crash deformations from FEA with damage evolution can better represent the crushing of the tube from experiment. Table 1 demonstrates comparison of the peak forces (P_{max}), the maximum displacements (d_{crush}) and energy absorption (EA) from experiment and the current FE models without and with damage evolution. It can be seen that the values for all key parameters are comparable with experimental data with some discrepancies in the peak force when damage evolution is not considered. This is due to the difference in failure behavior when damage evolution is implemented. In the model with damage evolution, crack and fracture mechanism can be observed at the top part of the tube. In contrast, the model without damage evolution shows no crack damage and failure occurs as folding of thin-walled member. Thus, it returns higher stiffness than the actual value.

4. Results and discussions

4.1 Direct Impact

A conical shell under direct axial impact is studied by using two material models as described earlier. Results of the deformed shapes from the two models as well as the initial peak forces, the mean forces and force-displacement curves are rather similar as shown in Fig. 8.

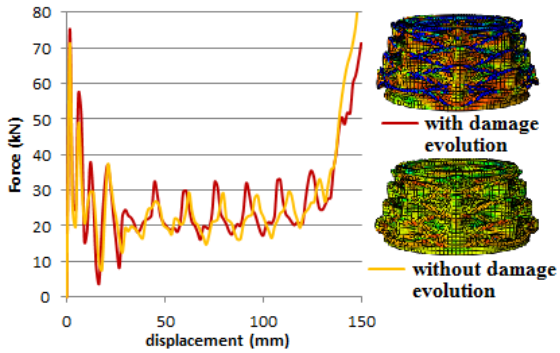

Fig. 8 Single-cell conical shell under direct impact

In direct impact of multi-cell conical tubes, Fig. 9 shows comparison of the mean crushing forces between the model with and without damage evolution for different multi-cell conical shells. It can be seen that as the numbers of cell increase, the use of model without damage evolution evidently overestimates the mean crushing force compared to the model with fracture damage.

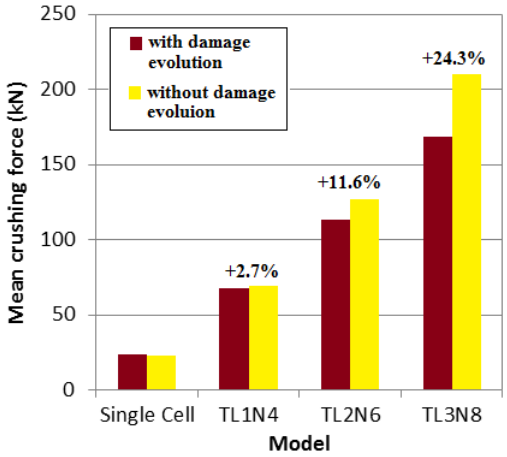

Fig. 9. Mean crushing forces for multi-cell conical tubes under direct impact

Fig. 10 displays an example of deformation configurations of the TL2N6 conical structure at 3 milliseconds and 9 milliseconds after impact obtained by using material model without and with damage evolution. Deformation patterns with 5 folding lobes along the circumference occur in both cases. However, folding develops along the entire length of the shell in model A without damage evolution (Fig. 10a). When damage evolution is introduced in model B, folding appears through only two-third of the shell length and the top part of the structure shatters and damages (Fig. 10b).

The difference in failure behavior is due to higher stiffness of the model without damage evolution when the shell undergoes large plastic strain since material degradation is not prescribed. In the model with damage evolution, the stiffness of the elements at the top part is softened when the plastic strains reach the prescribed criteria and the elements are removed when fracture displacement is reached. Therefore, the peak

force, mean crushing force and energy absorption of the model A without damage evolution are greater than those of model B.

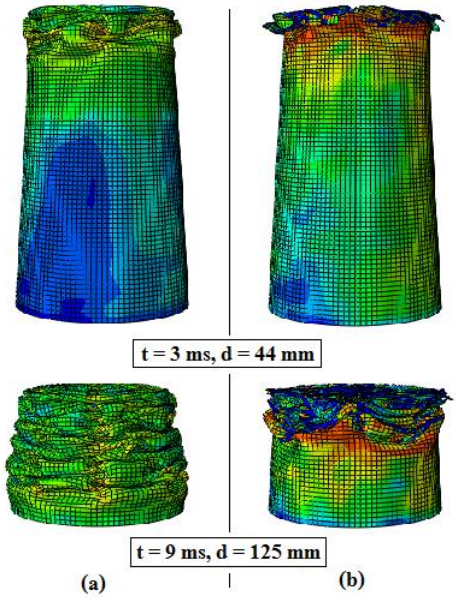

Fig. 10 Deformation patterns for TL2N6 under direct load (a) material model A without damage evolution (b) material model B with damage evolution

Table 2 listed the initial peak force (P_{max}) and mean crushing force (P_{mean}) of all single-cell and multi-cell tapered shells under direct axial load obtained by using model with damage evolution. The specific energy absorption (*SEA*) is computed at the same crushing displacement d_{crush} of 125 mm. It can be observed that the initial peak forces are increased when multi-cell structures are employed. However, the mean crushing forces and therefore the specific energy absorptions are considerably improved. Fig. 11 plots comparison of *SEA* with varying number of cell along the circumference (solid lines) and number of inside layer (dashed lines). It can be seen that when the number of cell along the circumference as well as the number of inside layer increases, the efficiency in crush absorption and *SEA* also increases.

Table 2 Energy absorption of different single-cell and multi-cell models

Model	*No. of cell*	*m* (kg)	P_{max} (kN)	P_{mean} (kN)	*SEA* (kJ/kg)
Single	1	0.11	75	2.98	27.9
TL1N4	5	0.20	130	8.67	44.5
TL1N6	7	0.21	132	9.70	45.8
TL1N8	9	0.23	150	11.3	49.1
TL2N4	9	0.26	172	12.4	48.0
TL2N6	13	0.28	191	14.7	52.2
TL2N8	17	0.31	206	17.4	57.1
TL3N4	13	0.32	215	16.5	51.9
TL3N6	19	0.34	242	18.5	53.9
TL3N8	25	0.37	254	22.0	59.5

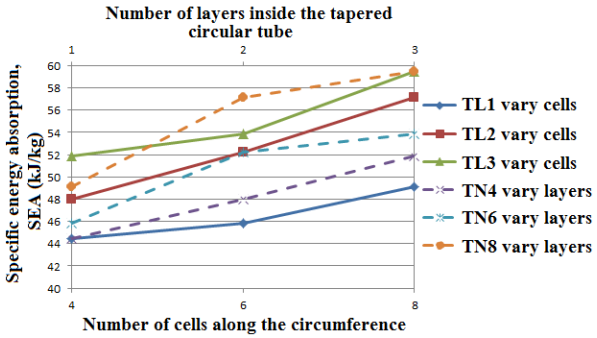

Fig. 11 *SEA* for tapered tubes with different numbers of cell along the circumference and numbers of layer

4.2 Oblique impact

Single-cell and multi-cell conical shells under 20-degree oblique load are studied by using material model with and without damage evolution. In most models, local buckling is observed at the top of the absorber followed by failure due to global buckling of the structure. Fig. 12 compares the specific energy absorption of single-cell and multi-cell thin-walled cones under oblique impact. Multi-cell conical shells are prone to global buckling under oblique load than the single-cell frusta especially when the number of cell increases since the cells act as stiffeners to the cone surface. In addition, when global buckling occurs, the specific energy absorption obtained from material model without damage evolution is only slightly larger than that from material model with damage evolution.

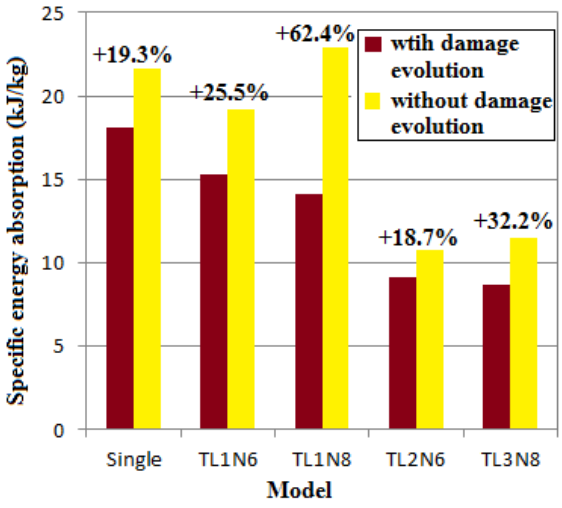

Fig. 12 SEA of conical tubes under oblique impact

Examples of deformation behaviors for TL2N6 at the time instances of 2.5 ms and 4.5 ms are depicted in Fig. 13. Material model without fracture mechanism gives an extremely large plastic strain of 1.74 at the base of the member. Since no fracture damage is defined, the shell is still intact with the bottom plate. In contrast, in the model with damage evolution, element deletion representing fracture failure is perceived at an early stage of impact. The member detaches from the base and thus the deformed angle of this model is

much larger than that of the former model. Buckling on the opposite side of the tube is more severe and the stresses and strains are larger than those from model A. Therefore, a lower value of energy absorption is attained when fracture is included.

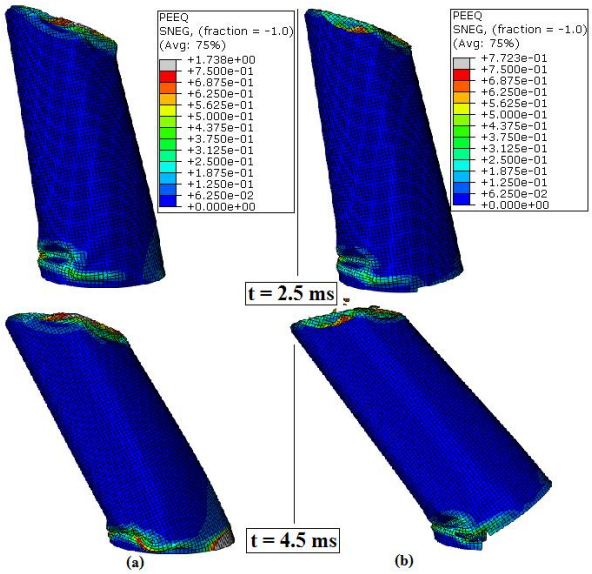

Fig. 13 Plastic strains and failure under oblique load of TL2N6 (a) Model without damage evolution (b) Model with damage evolution

5. Conclusions

The design of multi-cell thin-walled conical energy absorbers under dynamic impact is investigated based on dynamic explicit finite element analysis with and without progressive damage evolution formulation in the material model. For single-cell conical shells, the parameters including initial peak force, mean crushing force and specific energy absorption obtained from the two models are analogous. However, results from the material model without fracture damage can markedly overestimate specific energy absorption of multi-cell conical shells although the modes of failure are similar. Discrepancies are more prominent when the number of cell increases. Additionally, multi-cell conical tubes are shown to efficiently enhance the crashworthiness of the energy absorber under direct impact with awareness of possible global buckling when oblique impact occurs.

6. References

[1] Alavi, N.A. and Parsapour,M. (2014). Comparative analysis of energy absorption capacity of simple and multi-cell thin-walled tubes with triangular, square, hexagonal and octagonal sections, *Thin-Walled Structure*, Vol.74, pp. 155-165.

[2] Qiu, N., Jianguang, F., Zhaoxuan F., Guangyong, S. and Qing, Li. (2015). Crashworthiness analysis and design of multi-cell hexagonal columns under multiple loading case, *Thin-Walled Structure*, Vol.104, pp. 89-101.

[3] Tarlochan, F., Samer, F., Hamouda, A.M.S. and Karam, K. (2013). Design of thin wall structures for energy absorption application, *Thin-Walled Structure*, Vol.71, pp. 7-17.

[4] Alghamdi, A.A.A. (2001). Collapsible impact energy absorbers: an overview, *Thin-Walled structures*, Vol.39, pp. 189-213.

[5] Zhiliang, T., Shutian, L. and Zonghua, Z. (2013). Analysis of energy absorption characteristics of cylindrical multi-cell columns, *Thin-Walled Structure*, Vol.62, pp. 75-84.

[6] Xiong, Z., Gengdong C. and Hui, Z. (2006). Theoritical prediction and numerical simulation of multi-cell square thin-walled structures, Thin-Walled Structures, Vol.44, pp. 1185-1191.

[7] Ali, N. and Masoud, R.R. (2011). Mechanics of axial plastic collapse in multi-cell, multi-corner crush tubes, *Thin-Walled Structure*, Vol.49, pp. 1-12.

[8] Sajad, A., Abbas, R., Ali, G. and Hamed, M. (2015). Axial crushing analysis of empty and foam-filled brass bitubular cylinder tubes, *Thin-Walled Structure*, Vol.95, pp. 60-72.

[9] Cenk, K. (2015). Numerical crushing analysis of aluminum foam-filled corrugated single- and double-circular tubes subjected to axial impact loading, *Thin-Walled Structure*, Vol.96, pp. 82-94.

[10] Djamaluddin, F., Abduullah, S., Ariffin, A.K. and Nopiah Z.M. (2015). Optimization of foam-filled double circular tubes under axial and oblique impact loading conditions, *Thin-Walled Structure*, Vol.87, pp. 1-11.

[11] Chang, Q., Shu, Y. and Fanliang, D. (2012). Crushing analysis and multiobjective crashworthiness optimization of tapered square tubes under oblique impact loading, Thin-Walled Structure, 62, pp. 75-84.

[12] Shujuan, H., Xu, H., Guangyong, S., Shuyao, L., Wei, L., Xujing, Y. and Qing, L. (2011). Multiobjective optimization for tapered circular tubes, *Thin-Walled Structure*, Vol.49, pp. 855-863.

[13] Sheriff, M., Gupta N.K., Ramachandran, V. and Shamugpriyan , N. (2008). Optimization of thin conical frusta for impact energy absorption, *Thin-walled structures*, Vol.45(6), pp. 653-666.

[14] Hui, z. and Xiong, Z., (2016). Crashworthiness performance of conical tubes with nonlinear thickness distribution, *Thin-Walled Structure*, Vol.99, pp. 35-44.

[15] Yong, Z., Guangyong, S., Xipeng, X., Guangyao, L. and Qing, L. (2014) Multiobjective crashworthiness optimization of hollow and conical tubes for multiple load cases, *Thin-Walled Structure*, Vol.82, pp.331-342.

[16] Hooputra, H., Gese, H., Dell, H. and Werner, H. (2004). A comprehensive failure model for crashworthiness simulation of aluminium extrusions, International Journal of Crashworthiness, Vol.9, pp.449-463.